Feasibility Study of Green Hydrogen to Decarbonise New Zealand's Industries

Daniel Jia Sheng Chong, Michael Walmsley, Martin Atkins, Ahuroa Leach
Ahuora – Centre for Smart Energy Systems, School of Engineering,
The University of Waikato, Hamilton, New Zealand
e-mail: daniel.chong@waikato.ac.nz

ABSTRACT

Adopting renewable feedstocks is a transformative approach to diminish the reliance on fossil feedstocks such as natural gas and coal in the chemical industry. This research evaluates the potential for Aotearoa-New Zealand, particularly in the North Island, to harness green hydrogen production as a substitute for fossil fuels across industries. The study's scope encompasses examining renewable energy technologies, their capacity factors based on location, types of electrolysers, the conversion process, and the sizing of hydrogen storage reservoirs. An analysis of the levelized cost of hydrogen (LCOH) throughout the value chain in various scenarios has been conducted for the years 2020 to 2040 while considering the country's resource constraints. The issue is addressed through an optimization-based framework characterized by a multi-period, mixed-integer linear programming (MILP) model. The outcomes demonstrate the capability of integrating all these components within the mathematical framework to yield optimal solutions for transitioning towards a sustainable hydrogen economy.

KEYWORDS

green hydrogen, process network synthesis, process optimisation, renewable energy, hydrogen value chain

BACKGROUND

The global demand and consumption of energy are escalating exponentially as a result of the surge in population, the increase in affluence within developing countries, and rapid industrialisation. According to Sazali [1], fossil fuels which emit significant quantities of greenhouse gases contributing to climate change and global warming, fulfil 80% of the global demand for hydrogen in 2020. Henceforth, hydrogen and its derivatives have been under the spotlight as a potential fuel alternative to replace gasoline and natural gas as they prove to be an energy vector that can be stored and provide dispatchability whenever required.

The advocacy for the adoption of hydrogen is gaining popularity for several reasons [2]. Firstly, it can be integrated with renewable energy sources. Green hydrogen which is produced from clean energy through electrolysis is carbon zero and can be kept in reservoirs. Subsequently, it can be transformed back into electricity to meet peak load demands or further processed into chemical fuel for downstream applications. However, the focal point of green hydrogen is its role in industrial decarbonisation. Given that hydrogen gas serves as a carbon-neutral energy carrier, it can be utilized in a chemical process that employs hydrogen as a sustainable feedstock or as a key starting ingredient for decarbonisation.

Minimising the dependence on fossil fuels and shifting towards fuels with lower emissions constitutes a primary objective of Aotearoa New Zealand's Emissions Reduction Plan. The green hydrogen sector is anticipated to start on a small scale, yet it is projected to experience significant growth in the future once both investors and governmental entities recognise the potential and significance of incorporating hydrogen into the renewable electricity network [3]. Significant hydrogen-consuming chemical facilities, including plants for ammonia, methanol, and hydrogen peroxide, are situated in the Central North Island, specifically in the Taranaki region. Several challenges arise in the generation of green hydrogen from renewable energy, with the primary concern being the intermittency and spatial variability of solar and wind whereas geothermal is location-specific which implies that there was no certainty that hydrogen could be produced instantaneously and readily dispatched.

Extensive research has been conducted on addressing the hydrogen value chain in distinct levels of scenarios recently. Detailed depiction of the hydrogen network which encompasses various spatial details of the connections between hydrogen production, storage and end-user demand sites are explicitly defined to gauge the suitable selection of transportation modes and the state of hydrogen. Most of the case studies employ a mixed integer linear programming (MILP) approach to solve the permutation of pathways in the mathematical model [4], [5], [6], [7]. Henceforth, a geographic information system (GIS) tool is often employed to analyse and visualise geographically referenced data.

GIS methodology is employed to evaluate the production costs, potentials, and optimal locations for hydrogen and its derivatives, which include methanol, methane, and Power-to-Liquid (PtL) fuels [8]. The researcher was able to conduct suitability studies on various land factors such as land use, proximity to urban areas and facilities, and biological constraints on determining the optimal location for renewable power generation sites. Work presented by [9] coupled mathematical optimisation and GIS-based approaches to minimise the levelized cost of hydrogen by altering the sizing of electrolysers and modifying the sites of hydrogen

refuelling stations and grid connection. Pyomo optimisation tool was used for the mathematical operation. A case study in New Zealand on the technoeconomic study of the hydrogen supply chain was examined in 2021 by [9]. However, the scope of the work only focused on the green hydrogen supply network as a sustainable transportation fuel for heavy vehicle fleets. As a result, there is a significant gap in the feasibility study of New Zealand's hydrogen economy, indicating the need for further investigation in future research.

Being one of the pioneers in hydrogen supply chain modelling, [6] explored the optimal transition to commercial-scale hydrogen infrastructure within the transportation sector in the Netherlands. [10] focused on the optimization of hydrogen networks across Great Britain. The scope of research to include hydrogen pipelines and carbon capture and storage technologies was expanded by [11], with a focus on the total investment cost. On the other hand, some researchers have investigated the dynamics of hydrogen production with seasonal storage capabilities [12]. Samsatli and Samsatli [13] provided a more detailed examination of the hydrogen value chain across industrial, district heating, and electricity generation systems. They introduced a novel and comprehensive model that considers multi-step period operation and inter-seasonal storage options extending up to 2050. The model is further integrated with GIS to pinpoint optimal locations for wind and solar farms to meet hydrogen demand.

The present paper is structured as follows: Section 2 introduces the problem statement along with the potential hydrogen pathways. The mathematical model and process structure are elaborated in Section 3. The cost function, which includes the objective function and revenue, is outlined in Section 4. Section 5 focuses on the results and discussion of several timelines. Finally, the paper concludes with remarks on further improvements and the potential challenges of the research.

PROBLEM STATEMENT

The objective of this work is to design an optimal green hydrogen supply chain infrastructure for the prospect of delivering hydrogen to key chemical industries in the North Island region. Several scenarios projected to analyse the feasibility of the implementation of green hydrogen within the timeline from 2020 to 2040 while scrutinising several constraints in the model are the following:

Scenario 1. Electrolyser plants are operated off-grid, and the use of grey hydrogen is excluded from the work.
Scenario 2. Electrolyser plants are operated off-grid or on-grid, and the use of grey hydrogen is excluded from the work.
Scenario 3. Electrolyser plants are operated off-grid or on-grid, and the use of grey hydrogen with emission costs is included in the work.

The optimisation model addresses issues concerning the types of renewable energy used corresponding to their capacity factor and nameplate capacity, types and sizing of proposed electrolysers, capacity of hydrogen storage, conversion module for hydrogen pathways, transport modes selections and the combination of connection between hydrogen sources and demand centre. Besides that, the characterisation of SMR without carbon capture for hydrogen production is studied in the optimisation model. The historical data for the wholesale industrial price of electricity for the year 2022 are utilized for both Scenario 2 and Scenario 3, instead of

the year 2020. This adjustment is made because the data from 2020 are influenced by the pandemic, which could result in an inaccurate reflection of electricity pricing throughout the entire North Island Region.

The case studies elucidated within this paper offer valuable perspectives on the key questions and concerns about the hydrogen value chain are outlined as follows:

1. The interdependence among the amalgamation of renewable energy [13].
2. Interaction between renewable electricity generation with grid electricity network
3. Selection of electrolysers' type
4. Determination of storage location
5. Selection of storage facilities
6. Transportation mode and connectivity between generation sites, storage location and demand centres [11]
7. Selection of intermediate hydrogen pathways for storage and transmission
8. Cost comparison between green hydrogen and grey hydrogen as chemical feedstocks while accounting for carbon tax.

MATHEMATICAL MODEL

At the epicentre of the study, the hydrogen supply chain model is a single objective optimisation model which consists of a multiperiod MILP approach. The MILP model is formulated using Pyomo, which works proficiently in high-level analysis and optimisation tools [14]. The MILP optimisation framework is extremely efficient in several scenarios. In this study, multiple selection pathways are to be identified while simultaneously streamlining the design, planning and operation of the processes in each location site. These combinations are further complicated by considering the multiperiod response of each unique capacity factor of electricity generation at each location, leading to difference levelized cost of electricity for each site which would ultimately have implications for the hydrogen production profile and fluctuations in the hydrogen inventory storage.

With the help of the optimisation framework, the cost effectiveness of various hydrogen conversion pathways will be discovered, which answers the most optimal way of processing hydrogen to cater for its transportation and storage facilities. Ultimately, the model has been developed to propose the configurations of production, storage and distribution of hydrogen infrastructure at different timelines to study the feasibility of green hydrogen in Aotearoa-New Zealand's hydrogen economy. The network model also includes current practice of hydrogen production method in the chemical industries which is SMR, to examine the influence of carbon prices on the transition to a net zero economy with different timelines.

By delineating expenditures related to renewable sources, grid infrastructure, electrolyser, transportation, storage, process technologies and costs associated with SMR, stakeholders can gain insights into where resources are allocated and identify potential areas for optimization or cost-saving measures. Additionally, such a breakdown of infrastructure costs aids in a better decision-making process by enabling stakeholders to prioritise investments, allocate resources efficiently, and assess the overall economic viability of the system or project.

Model Overview

The comprehensive hydrogen value chain model attributes time intervals to portray the flow of quantity in each process system. The time interval comprises the monthly planning period for a year. Hence, the period $t \in T$ is subject to be a subset of a set consisting of 12 elements to express each month. The superstructure is first developed by defining each spatial-explicit location which is a series of electricity generation sites with built-in electrolyser plants, storage locations and demand centres. All 29 potential generation sites for hydrogen production are represented by location $i \in I$, where $\sum_i n_i^i = 29$. The storage locations are represented by $j \in J$ which consists of 4 potential storage sites in the North Island. The specific representations and process overview of each technology in each location are described in detail in the **Conversion Processes Subsection**.

Renewable Source

Wind and solar energy generation methods are classified as non-dispatchable, indicating that their electrical output cannot be easily adjusted or controlled to align with varying demand levels [15]. Consequently, they cannot promptly adapt to changes in load capacity. These renewable energy sources depend heavily on geographical factors, weather conditions, climate, and seasonal variations, making it challenging for them to consistently meet electricity needs during periods of peak demand. Conversely, geothermal energy is dispatchable. Hence, the unique characteristics of wind and solar energy, which have varying periods of intermittency, combined with geothermal energy's capability to provide a stable baseload power supply, underscore the importance of investigating the synergistic effects of these three renewable sources within the Power-to-Hydrogen (PtH) framework [16]. Therefore, the case study incorporates the analysis of operational and planned wind, geothermal, and solar energy projects within the generation model, offering insights into how these diverse renewable sources can be integrated to enhance the overall efficiency and reliability of hydrogen production.

The types of renewable technology $r = \{Wind, Solar, Geothermal\}$ attributes to the capacity factor CF_{irt}, along with generation site i and time t. The combination of different sets would provide unique values for the accuracy on quantification of resource (i.e electricity and hydrogen) which ascertain the quality of the modelling results from the optimisation framework.

Renewables.ninja platform is utilised to simulate wind power production and to determine the capacity factors related to solar irradiance at the production sites because Renewables.ninja has access to reliable wind speed and solar irradiance data. The platform's data for wind and solar are derived from NASA's Modern-Era Retrospective Analysis for Research and Applications, Version 2 (MERRA-2) global reanalysis model. MERRA-2 is known for producing fairly accurate results, which have been validated by several countries [17], [18], [19]. Although there is no specific literature validating its data for New Zealand, the information obtained from Renewables.ninja for the 29 locations studied aligns well with solar irradiance data from the Global Solar Atlas and wind speed data from the Global Wind Atlas. The minor congruence between both outputs suggests that Renewables.ninja provides a reliable basis for assessing the renewable energy potential at these New Zealand locations. Moreover, Renewables.ninja is an open-source platform and its datasets are accessible to the public [20].

To estimate the required number of turbines at each potential wind farm, Vestas V47 660 kW turbines are assumed to be the standard, reflecting their use in New Zealand's largest wind farm, Tararua [21]. The median Global Horizontal Irradiance (GHI) for consented and proposed utility-scale solar farms is found to be 3.95 kWh/m^2 per day, suggesting that these solar farms align with Resource Class 9. The relatively low solar irradiance is indicative of placing the generalised solar farms in Resource Class 9 [22]. It is assumed that for geothermal energy, the newly proposed geothermal resources will utilise binary plants, which can convert lower temperature geothermal resources into electricity more efficiently than traditional flash steam turbines. The total expenditure cost of renewable generation plant is illustrated in Equation (1):

$$TOTEX^{renewable} = \sum_{i\in I}\sum_{r\in R}\sum_{t\in T} FIR_{i,r,t}^{rated} \cdot LCOE_{i,r} \quad (1)$$

Electrolysers

Electrolysis is an electrochemical process that applies direct current to conduct a non-spontaneous reaction. The principle of electrolysis is to convert electricity energy into chemical energy by dissociating water into hydrogen and oxygen gas. The overall chemical equation is illustrated as:

$$H_2O \rightarrow H_2 + 0.5O_2 \quad \Delta H = 33.33kWh/kg \quad (2)$$

Based on the literature, the resulting equation which represents the investment of electrolyser plant in USD/kW is shown in Equation (3) [23]. Since the Equation (3) is a non-linear curve fitting equation which describes a series of datapoints generated and projected by several sources, standard errors with their coefficients for both proton exchange membrane (PEM) electrolyser and alkaline water electrolyser (AEL) are detailed in Table 1.

$$invest_{i,e}^{ie} = \left(k^0 + \frac{k}{Cap_{i,e}^{ie}} \cdot {Cap_{i,e}^{ie}}^{a}\right)\left(\frac{V}{V^0}\right)^{\beta}, \qquad \forall i \in I, \forall e \in E \quad (3)$$

Where $invest_{i,e}^{ie}$ denotes the total investment cost of the electrolyser plant per kW $Cap_{i,e}^{ie}$ is the electrolyser plant capacity in kW, V and V^0 attributes to the studied year and the referenced year, k^0 and k are coefficient constants, while a and β express the scale factor and learning rate of the electrolyser respectively.

Table 1. Coefficient for PEM electrolyser and AEL [23].

Parameter	a	β	k^0	k	V^0	Standard error
AEL	0.649	−27.33	301.04	11,603	2020	547
PEM electrolyser	0.622	−158.9	585.85	9,458.2	2020	510

Most optimisation problems are illustrated as mixed integer and non-linear (MINLP) approaches in engineering calculations. Despite MINLP able to produce better approximations for an optimal solution, it is still limited to smaller problems. Hence, an efficient piecewise linear function is implemented for the non-linear equation which reduces the computational time with bearing considerable approximation errors. Hence, the non-linear Equation (4) will be represented as:

$$invest_{i,e}^{ie} = \begin{cases} m_1 \cdot Cap_{i,e}^{ie} + c_1, & a_1 < Cap_{i,e}^{ie} \leq b_1, \forall e \in E \\ m_2 \cdot Cap_{i,e}^{ie} + c_2, & a_2 < Cap_{i,e}^{ie} \leq b_2, \forall e \in E \\ m_n \cdot Cap_{i,e}^{ie} + c_n, & a_n < Cap_{i,e}^{ie} \leq b_n, \forall e \in E \\ & \dots \end{cases} \quad (4)$$

Apart from different cost functions used in the model as economies of scale, the Equation also accounts for the projection year of both technologies. As affirmed by literature, PEM electrolyser is less mature, thus PEM has a higher learning rate of 13%, therefore has a higher potential for cost reduction whereas AEL has a learning rate of 9% due to its considerably developed technology as proposed by the [24]. The model also assumes a 0.25% annual improvement in system efficiency for PEM electrolysers, in anticipation of advances in research and development [25]. Additionally, an overload capacity of 150% for up to 20% of the total operational time is considered for electrolysers [26]. The inclusion of overload capacity allows for temporary operation above the nameplate capacity without compromising the lifespan of the electrolyser stack.

The electrolyser technology, E is depicted with the subset $e \in E$, where $E = \{AEL, PEM\}$. Only two types of electrolysers are considered in the optimisation framework as PEM and AEL are the more promising electrolysers that will be employed in large scale operations in the transition period from fossil fuels to a decarbonisation economy.

Transport

Hydrogen can be transported in its pure form, either as compressed gas in pipelines or trailers, in liquid cryogenic form, or converted into hydrogen carriers such as Liquid Organic Hydrogen Carriers (LOHC). The transport mode, Tr is denoted with the set $Tr = \{CH_2\ trailer, LH_2\ trailer\ \ , LOHC\ trailer, CH_2\ pipelines\}$. In the model, it is often combined with storage options at storage location at a certain time period which is defined with the subset $J\ Tr\ St\ T\ \subseteq J\ \times Tr\ \times St\ \times T$. The combination of subset is to define attributes for a variable for resource balance and cost function purposes. The superstructure of hydrogen between each location is summarised in Figure 1. Figure 1 denotes the transportation links between generation sites and storage locations, as well as between generation sites and demand centres, and finally, between storage locations and demand centres. The visual representation helps in understanding the logistical and infrastructural relationships within the hydrogen supply network, highlighting the pathways through which hydrogen is produced, stored, and allocate the synthesised hydrogen to its respective demand.

The mass balance for the transportation network from the source will be represented in Equation (5). The amount of hydrogen from each production site with transport tr at time t is equal to the sum of flow of connection from production site i to intermediate storage location j using transport tr at time t and the sum of flow of connection from production site i to demand centre k using transport tr at time t.

$$FITr_{i,tr,t} = \sum_{j \in J} FIJTr_{i,j,tr,t} + \sum_{k \in K} FIKTr_{i,k,tr,t}, \quad \forall i \in I, \forall tr \in Tr, \forall t \in T \quad (5)$$

The Equation (6) will outline the mass balance for the transportation network at the demand centre. It is expressed as the quantity of hydrogen delivered using transport mode tr to demand centre k at given time t is equal to the total of the flow from production site i to demand centre k via transport tr at time t plus the total flow from storage site j to demand centre k using transport tr at time t.

$$FKTr_{k,tr,t} = \sum_{j \in J} FJKTr_{j,k,tr,t} + \sum_{i \in I} FIKTr_{i,k,tr,t}\,, \qquad \forall k \in K, \forall tr \in Tr, \forall t \in T \qquad (6)$$

The transport module is subdivided into two calculations to express the differences in working out the delivery cost and payload capacity of the pipeline system and trailer systems respectively. Although pipeline transportation requires large initial investments, it has low operational costs once the infrastructure has been established. Moreover, pipeline infrastructures have a significantly longer operating lifespan than moving vehicles which potentially lowers down the annuity factor of the technology. On the other hand, operating and maintenance costs account for expenses associated with maintaining the pressure of the pipelines and repair costs by corrosion. The assumptions for transport modes and trucks' specifications are displayed in

Table A 3 and Table A 4.

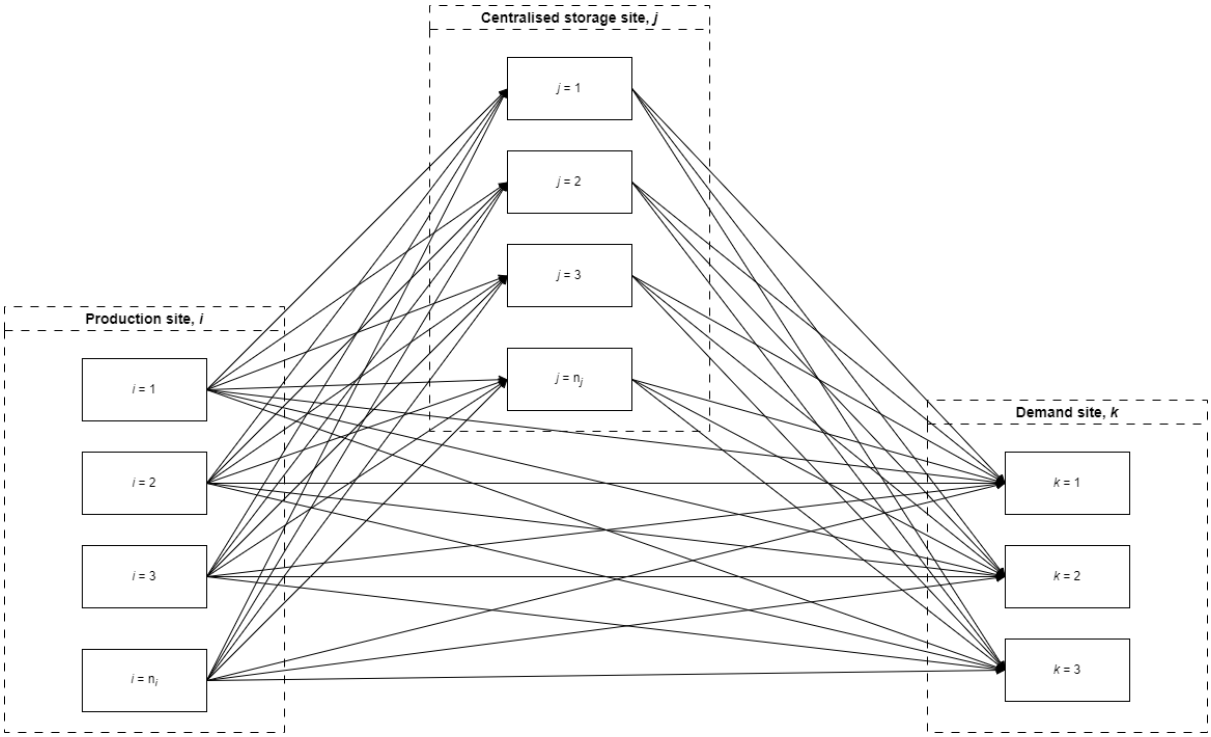

Figure 1. Superstructure of green hydrogen network between each location.

Storage

A physical storage system can withstand pressure as high as 700 bar for compressed hydrogen gas storage module. The cost of compressed hydrogen gas storage is constrained by the sizing of the vessel and the types of alloys used. In high-pressure conditions, the energy density (MJ/m^3) of hydrogen gas will increase significantly as the specific volume required decreases. However, a thicker wall of the storage vessels is required to withstand the pressure acting within the container. The wall thickness accounts for further capital expenditure when designing vessels while increasing the operating cost which is attributed to the additional compression required to maintain the set point pressure. Hence, exceedingly high-pressure storage modules are not recommended unless land availability is the limiting factor. In general, hydrogen gas is economically stored at 100 bar in surface-level containers [27]. In addition, the achievable hydrogen storage density at 100 bar is 7.8 kg/m^3 whereas the achievable hydrogen storage density at 200 bar is approximately 13 kg/m^3 [27].

The main benefit of liquefaction is it has a high density of 70 kg/m^3 at 1 bar [28]. Liquid hydrogen is one of the most promising hydrogen storage technologies as it is gravimetrically and volumetrically efficient for storage and transportation. However, the storage tanks must be insulated to maintain a cryogenic temperature. Hence, the storage vessels are double-walled and vacuumed to minimise heat transfer from the environment [29]. Liquefied hydrogen is susceptible to evaporation due to heat leakage. In the account of losses, boil-off rate of 0.03% per day or 3.74% per month is assumed for the storage of hydrogen liquefaction. LOHC is a practical alternative for chemical storage. LOHC is inherently more stable than diatomic hydrogen due to its physical properties as it exists in a liquid state in ambient conditions.

LOHCs are unsaturated organic compounds which bond with hydrogen particles during hydrogenation and release hydrogen when it is required. It has a high gravimetric storage density, accounting for approximately 6 wt% of the LOHC mixture (Niaz et al., 2015).

Three types of storage technologies are considered which is $St = \{GH_2$ Tank, LH_2 Tank, LOHC Tank$\}$. Some notable variables which are the subset of storage include $I_{j,st,t}^{FJSt}$ that is used to record the inventory balance for storage facility st at storage site j at time t. The net rate of utilisation of inventory storage is:

$$I_{j,st,t}^{FJSt} = \begin{cases} FJSt_{j,st,t}^{in} - FJSt_{j,st,t}^{out}, & \forall j \in J, \forall st \in St, t = 1 \\ (I_{j,st,t-1}^{FJSt} + FJSt_{j,st,t}^{in} - FJSt_{j,st,t}^{out}) \cdot X_{st}^{loss}, & \forall j \in J, \forall st \in St, t > 1 \end{cases} \quad (7)$$

Where the hydrogen inventory is the balance between the injectability or influx of hydrogen flow into the storage site $FJSt_{j,st,t}^{in}$ against the discharging rate of hydrogen from the storage site $FJSt_{j,st,t}^{out}$. It is assumed that there is no hydrogen stored in the inventory at the first-time interval. Hydrogen losses (predominantly boil-up rate) are considered for second-time interval onwards. The maximum capacity of hydrogen storage site is denoted by:

$$I_{j,st,t}^{FJSt} \leq I_{j,st}^{Cap}, \qquad \forall j \in J, \forall st \in St \quad (8)$$

Geographic information system (GIS) modelling

GIS is used to apply relevant factors for inclusion while scrutinizing restrictive factors for the exclusion of certain zones. The use of GIS aids in the decision-making process by filtering out unsuitable zones for hydrogen storage. For the geospatial work, ArcGIS Pro software is employed for managing, analysing, and visualising spatial data that was obtained from different sources. Table 2 illustrates the criteria for site selection while displaying all sites that were included in the study.

Table 2. Restrictive and determining factors for site selection.

Criteria	Description	Characteristics	References
Elevation	50-500m above sea level	Inclusion	[30]
Road networks	1km buffer	Inclusion	[30]
Urban centre	5km buffer	Exclusion	[31]
Water bodies	1km buffer	Exclusion	[30]
Protected areas	1km buffer	Exclusion	[30]
Coastlines	1km buffer	Exclusion	[30]
Fault lines	5km buffer	Exclusion	[32]

The restrictive and determining factors for site selection are discussed in the following. Table 3 presents the methodology required to identify the regions and sites suitable for storage. The blue shaded region in Figure 2 represents a feasible location site for intermediate storage modules.

Elevation — The elevation of the centralised storage site is set to be lower than 500 meters above sea level because there is difficulty in transporting hydrogen through elevated regions.

Road networks — Hydrogen storage sites must be maintained at least 1 km from the main road network. The proximity of the road to the hydrogen storage location makes it more accessible for transportation and fuelling purposes.

Urban centre — A 5 km distance away from the urban area must be maintained as a site selection criterion to prevent the adverse risk of fire and explosion caused by the hydrogen storage site due to mishap.

Water bodies — Zone within 1km of water bodies are excluded from the site selection. The exclusion is to reduce water pollution of water sources. Lakes, rivers, and streams are considered in this category.

Protected areas — A boundary layer of 1km from the protected zone has been instilled in the site selection matrix. Protected areas include forest reserves, marine areas, conservation areas, wilderness, wetlands, national parks etc.

Coastlines — It is necessary to build a hydrogen storage site 1km away from coastlines for safety purposes and to act as a buffer to most marine reserve sanctuaries.

Fault lines — It is advisable to build hydrogen storage sites away from fault lines which would also imply a higher likelihood of natural disasters.

Table 3. Summary of the methodology for obtaining the results.

Step	Description
1	Obtain and import different data sources into ArcGIS Pro
2	Convert exclusion and inclusion zone data into polygons
3	Import ArcPy package to perform geographical data analysis in Python Programming Language
4	The project raster tool is used to allow snap raster and to calibrate coordinate systems which are imported from ArcGIS Pro.
5	The clip raster tool is used to correct the extents of the snap raster
6	Set the minimum extent of the raster and cell size for each GIS file for spatial analysis
7	Create truth tables for the exclusion and inclusion of criteria
8	Reconvert and export output file into ArcGIS Pro for visual analysis and validation

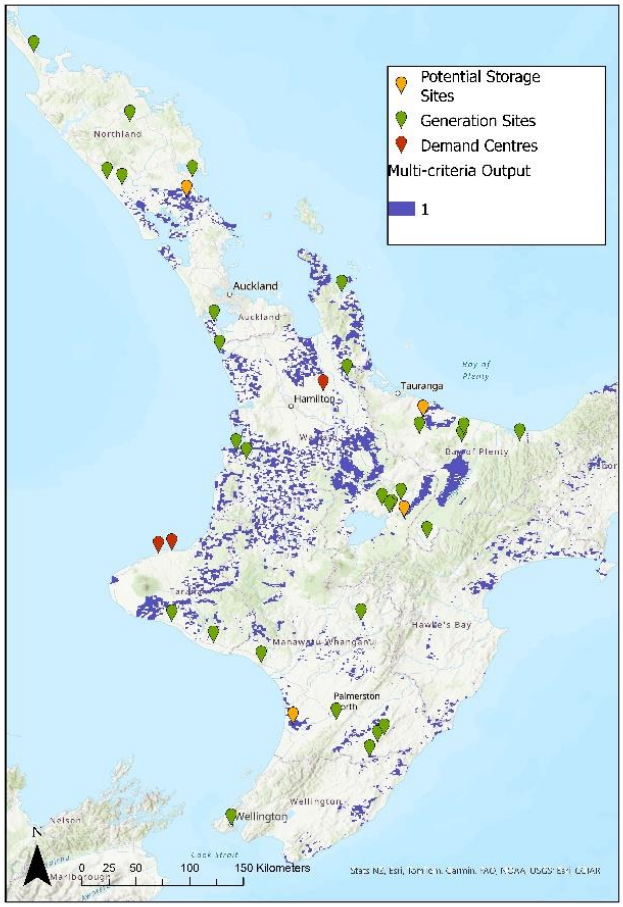

Figure 2. Possible generation sites, proposed storage locations and demand locations.

Conversion Processes

The hydrogen supply chain model elucidates key processes which convert the physical and chemical characteristics of green hydrogen to match its respective transportation, storage, and distribution technologies. As a summary of the model, hydrogen could exist in three states: gaseous, liquid cryogenic or bonded with LOHC. Various pathways are explored to determine the most efficient configuration of the hydrogen value chain. The conversion modules can be divided into three main sections: generation sites, storage sites, and demand centres. The assumptions on the specifications for each conversion module including energy and heat requirements as well as conversion losses are displayed in Table A 6.

Generation sites:

As hydrogen is produced in gaseous form from the electrolyser at a specific location, there are two available processes to change its chemical and physical properties. The process step 1 could be summarised as $P_1 = \{Nil, Liquefaction, Hydrogenation\}$. If a hydrogen production route does not require any operation to change its state, the element 'Nil' is assigned to that specific route. The significance of including P_1 is to account for the conversion losses associated with each process and the corresponding costs for each system.

Pressurisation is necessary before hydrogen can be loaded into trailers or pipelines for transportation. It is important to note that the type of pumps and compressors are exclusive to

the state of the hydrogen. Compressed hydrogen gas can be transported via two main methods: pipelines and trailers. On the other hand, liquefied hydrogen (LH_2) and LOHC require their specific types of trailers for transportation. Thus, the second process step is represented as $P_2 = \{Compression, LH_2\ pump, LOHC\ pump\}$, indicating the necessary steps for preparing hydrogen in different forms for transportation.

Storage sites:
The physical state of hydrogen entering the centralised storage site is based on its delivery mode. Further reconversion and conversion must be carried out to match the designated storage technologies. In the model, only one storage technology is deployed in every storage location. For instance, if the state of hydrogen delivery is the same as its storage module, process steps 3 and 4 are omitted. Conversely, the hydrogen must be reconverted to its gaseous state and undergo further conversion to match its long-term storage purposes. Referring to Figure 3, process step 3 denotes the reconversion process of liquefied hydrogen and LOHC by evaporation and dehydrogenation stages. Process step 3 could be represented as $P_3 = \{Nil, Evaporation, Dehydrogenation\}$. In process step 4, the superstructural network layer illustrates the conversion of hydrogen into the respective state before storing them in a centralised above-ground hydrogen reservoir. Like process step 2, process step 4 is depicted as $P_4 = \{Nil, Compression, LH_2\ pump, LOHC\ pump\}$. However, the "Nil" element is added to the set as it allows the process to bypass if the state of hydrogen does not require any changes from transportation to storage.

Demand sites:
Similar to the situation at the receiving end of the storage site, the hydrogen has to undergo reconversion to accommodate the process operation of the chemical industries. Hydrogen in the gaseous state is well-suited as feedstock in the chemical industries namely methanol, ammonia, and hydrogen peroxide manufacturing processes. Hence, liquid hydrogen and LOHC transmitted from trailers have to be evaporated and dehydrogenated to their original state which compressed hydrogen could be readily available for use without reconversion. Process step 5 is presented as $P_5 = \{Nil, Evaporation, Dehydrogenation\}$. The hydrogen carrier will be delivered back and recycled to transport hydrogen from the production and distribution site. Grey hydrogen which derives from conventional natural gas sources, is available from steam methane reforming without carbon capture to cater for the hydrogen requirement at each demand centre. The amount of carbon emitted will be calculated to account for the carbon emission cost. Additional conversion process is necessary to change the state of transported hydrogen to a suitable state to be used as chemical feedstocks in the industrial plant.

Equation (9) refers to the amount of hydrogen demand equals to the sum of transported hydrogen with hydrogen manufactured from steam methane reforming.

$$DEM_{k,t} = FK_{k,t} + FK_{k,t}^{SMR}, \qquad \forall k \in K, \forall t \in T \tag{9}$$

The total annual amount of hydrogen demand is:

$$DEM^{Total} = \sum_{t \in T} \sum_{k \in K} DEM_{k,t} \tag{10}$$

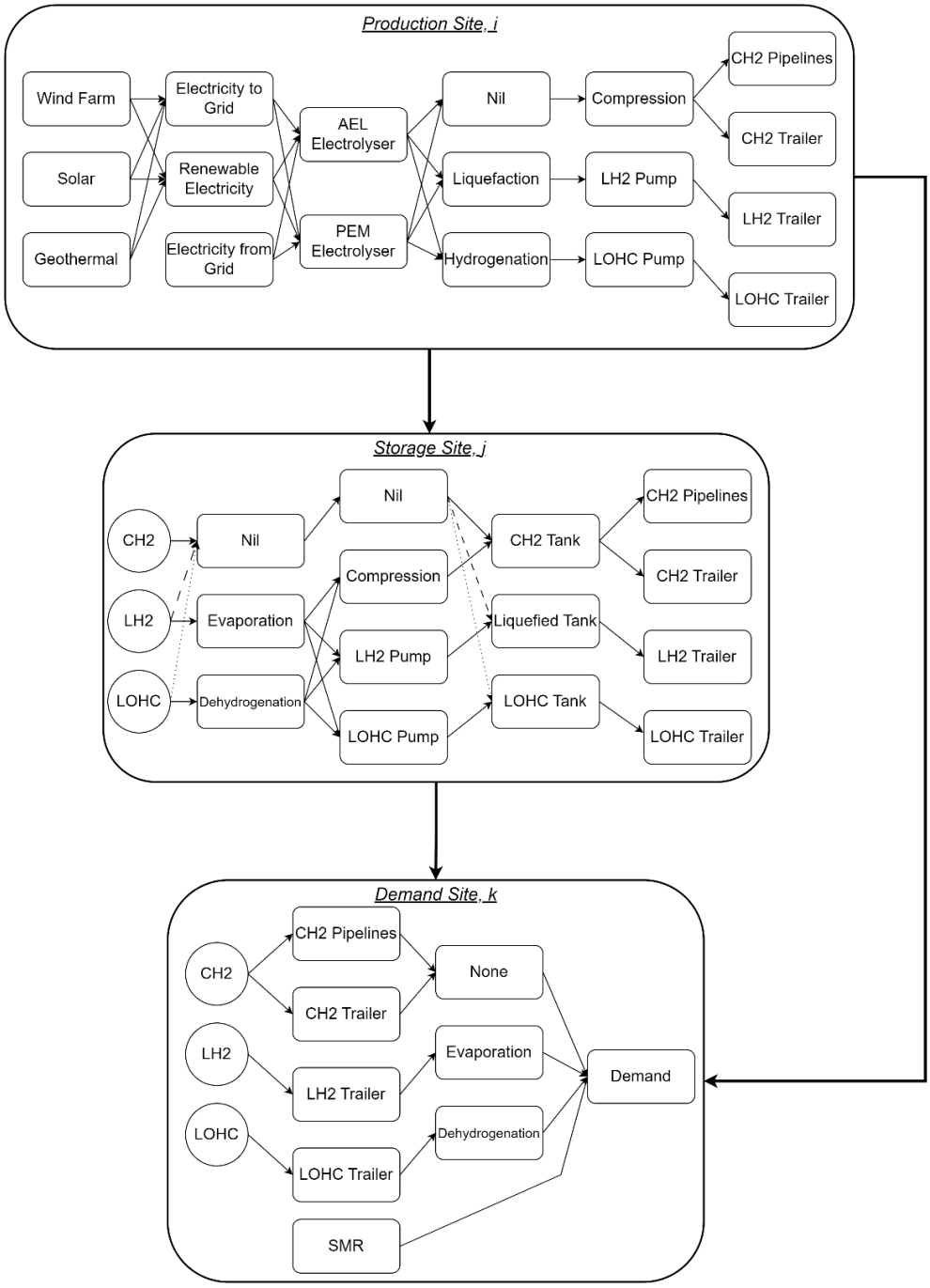

Figure 3. Network superstructure of the hydrogen value chains, illustrating all potential hydrogen pathways within each system and delineating site boundaries. Dotted and dashed lines in the diagram signify the selected pathways based on the physical state of hydrogen.

COST FUNCTION

Objective Function

The optimisation framework seeks to minimise the cost of hydrogen production, storage, and distribution by systematically analysing variables, parameters, and constraints to produce a feasible solution. Equation (11) provides a detailed breakdown of the total expenditure ($TOTEX$) into its constituent parts, allowing for a comprehensive analysis of the costs

associated with different aspects of the system under consideration. The notations and abbreviations are listed in the NOMENCLATURE Section.

$$\begin{aligned} TOTEX = {} & TOTEX^{renewable} + TOTEX^{grid} + TOTEX^{etech} + TOTEX^{truckij} \\ & + TOTEX^{transportij} + TOTEX^{truckjk} + TOTEX^{transportjk} \\ & + TOTEX^{truckik} + TOTEX^{transportik} + TOTEX^{store} + TOTEX^{p1} \\ & + TOTEX^{p2} + TOTEX^{p3} + TOTEX^{p4} + TOTEX^{p5} + TOTEX^{smr} \end{aligned} \quad (11)$$

General Cost function:

For the sizing of the capacity of an equipment or system, it is worth considering the overcapacity factor f^{cap} to increase the flexibility of the process to deliver the projected amount of hydrogen despite facing unscheduled downtime of the plant. Moreover, as the model accounts for the hydrogen losses in the few step processes and conversion modules, an overproduction factor f^{prod} is considered in the sizing of a system [33].

$$Capacity^{eq} = Capacity^{eq,nominal} \cdot f^{cap} \cdot f^{prod} \quad (12)$$

The investment cost of equipment is often adjusted to account for the sizing of the capacity. The general rule for cost exponents uses a scale factor to estimate resulting investment cost with different throughput which is referenced to an equipment with known investment costs.

$$Invest^{eq} = Invest^{ref} \left(\frac{capacity^{eq}}{capacity^{ref}} \right)^{scale\ factor} \quad (13)$$

As a non-linear programming (NLP) model rarely provides a converged global optimal solution or obtains a feasible solution, the non-linear Equation (13) undergoes relaxation into a piecewise MILP term in Equation (14) to reduce the computation time and complexity of the problem.

$$Invest^{eq} = \begin{cases} m_1 \cdot capacity^{eq} + c_1, & a_1 < capacity^{eq} \leq b_1 \\ m_2 \cdot capacity^{eq} + c_2, & a_2 < capacity^{eq} \leq b_2 \\ m_n \cdot capacity^{eq} + c_n, & a_n < capacity^{eq} \leq b_n \\ \ldots & \end{cases} \quad (14)$$

An annuity factor AF is a financial concept that determines the net present economic value of any future financial instrument. Annuity factor AF is applied to evaluate the specific annual capital expenditures. Annuity factor AF is a function of depreciation period n and the Weighted Average Capital Cost ($WACC$).

$$AF = \frac{(1 + WACC)^n \cdot WACC}{(1 + WACC)^n - 1} \quad (15)$$

The $CAPEX^{eq}$ for a given module could be illustrated by including the annuity factor AF and overproduction factor f^{prod} with the investment cost.

$$CAPEX^{eq} = \frac{Invest^{eq} \cdot AF}{f^{prod}} \quad (16)$$

The $OPEX^{eq,fix}$ is expenses associated with the fixed operating expenses and maintenance cost in the process. $OPEX^{eq,fix}$ is not affected by the throughput of the process and remains constant to ensure a day-to-day operation.

$$OPEX^{eq,fix} = \frac{Invest^{eq} \cdot OM^{fix}}{f^{prod}} \quad (17)$$

The $OPEX^{eq,var}$ represents the utility costs such as natural gas, electricity, fuel, and water as well as feedstock costs which are influenced by the amount of throughput at a specific point of time.

$$OPEX^{eq,var} = throughput \cdot electricity\ demand^{ref} \cdot electricity\ price^{ref} + throughput \cdot heat\ demand^{ref} \cdot heating\ price^{ref} \quad (18)$$

The total overall expenditure for one module $TOTEX^{eq}$ represents the sum of $CAPEX^{eq}$, $OPEX^{eq,fix}$ and $OPEX^{eq,var}$.

$$TOTEX^{eq} = CAPEX^{eq} + OPEX^{eq,fix} + OPEX^{eq,var} \quad (19)$$

RESULTS AND DISCUSSION

The mathematical model was adapted for three case studies to assess the impact of the hydrogen supply chain network within the timeline from 2020 to 2040. Each optimization model is composed of roughly 2084 constraints and 1132 variables, and it can be resolved in under 10 minutes. All optimization models utilize the Gurobi Mixed-Integer Programming (MILP) solver, which applies an advanced, cutting-edge branch-and-cut algorithm. The computations are performed on a 12th Gen Intel(R) Core (TM) i7-12700H processor, clocked at 2.30 GHz, with 32.0 GB of installed RAM.

Comparison between Scenario 1 and Scenario 2

In Scenario 1, the demand for renewable electricity for producing green hydrogen substantially exceeds that in the second scenario, which utilizes grid electricity for electrolysis. The findings from 2020 reveal that the levelized cost of hydrogen in Scenario 1 is NZD27.82/kgH_2, and in Scenario 2, it is NZD8.21/kgH_2. This significant disparity can be attributed to differences in storage and transportation costs. Specifically, the higher costs in Scenario 1 are due to the total investment required for storing energy in a physical form (i.e., hydrogen), which is more expensive as new hydrogen storage infrastructures significantly contribute to capital and operating expenses. Additionally, hydrogen losses present a challenge for cryogenic hydrogen storage systems, necessitating more electricity and larger electrolyser sizing to compensate for the losses due to boil-off.

Centralized storage can store excess hydrogen to counteract the inconsistency of renewable energy sources, such as wind and solar power. However, this approach necessitates the creation of larger electrolyser capacities and power generation installations. According to the results, cryogenic hydrogen storage emerges as the most viable method for long-term hydrogen storage, despite constituting 40% of the total levelized cost of hydrogen. Nonetheless, this method is highly uneconomical, as hydrogen storage facilities remain underutilized for most of the period. Figure 4 illustrates the storage profile of liquefied hydrogen at the storage site in Taupo Region.

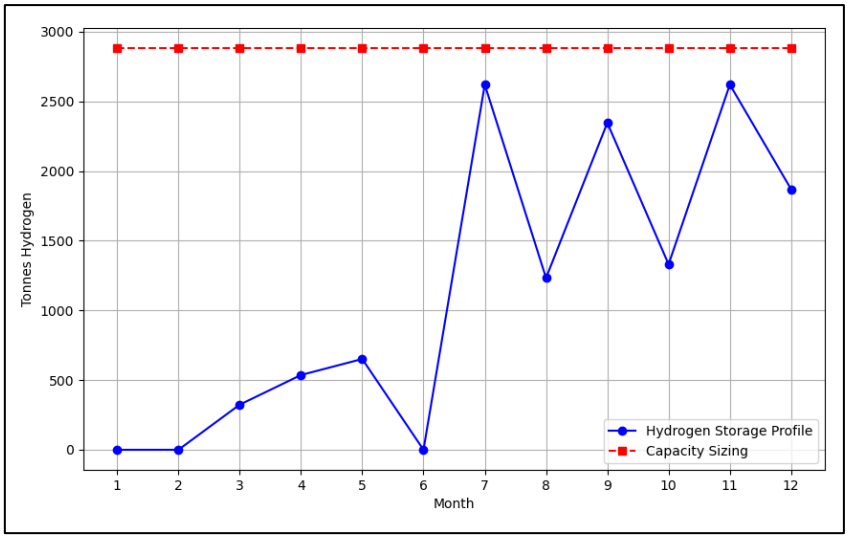

Figure 4. The storage profile for liquefied hydrogen in site $j = 3$ (Taupo Region)

The increase in equipment sizing from the fluctuation from generation will increase the capital cost of hydrogen infrastructure which will ultimately increase the levelized cost of hydrogen despite supplying an equal amount of hydrogen in other scenarios. Moreover, Scenario 1 highlights the significant role of geothermal electricity production, valued for its steady baseload power, which ensures a high utilization factor for the electrolyser. The baseload characteristics by geothermal energy able to stave off distinct fluctuations from intermittent wind and solar generation, ultimately reducing the volume of storage capacities of all sites. In contrast, utilizing on-grid electricity in Scenario 2 allows for maintaining electrolyser stability, enabling it to operate at optimal capacity for most of the time. Furthermore, distinct from other countries with stable electricity prices year-round, New Zealand experiences electricity price fluctuations at 30-minute intervals. The generation variability introduces periods when the wholesale electricity price dips below that of renewable technologies, presenting a strategic advantage despite potentially higher grid electricity costs during some months. The compromise involves adjusting the size of the plants based on on-grid electricity usage. Consequently, with grid-sourced electricity, there is no need for transporting green hydrogen to storage sites, as hydrogen is produced on demand and directly supplied to the chemical industries. Therefore, it can be observed that Scenario 2 has higher cost for electricity resources, which a sum of renewable energy expenses and grid costs whereas the cost for electricity resources is only comprised of renewables in Scenario 1.

Regarding transportation methods, both scenarios utilize pipeline transportation and LOHC trailers. Pipeline transportation is preferred for transporting high loads over long distances, while LOHC trailers are more cost-effective for moderate loads over shorter distances. Notably, LOHC is generally more affordable than options for cryogenic hydrogen transport and compressed gas trailers, despite the need for reconversion at the destination through dehydrogenation process. Given its cost-efficiency, hydrogen is favoured to be transported in a liquefied state directly from cryogenic storage sites to minimize reconversion costs. In both cases, however, AEL is a more economical way for hydrogen production in large scale operations in 2020 but a transition to PEM electrolysers could be observed in 2040. The results also indicate that transportation costs play a significant role in the affordability of hydrogen. Consequently, in cases such as Scenario 2, most hydrogen generation sites are strategically

allocated near demand centres as the stability of the demand flow is resolved with grid electricity. Therefore, the existence of centralised storage is redundant in Scenario 2. The location proximity between production and hydrogen consumption minimises transportation distances, which in turn reduces costs by 70 percent from Scenario 1 to 2 which makes hydrogen much more economically feasible for end users. Moreover, fewer trips have to be taken as the travel to and from storage sites are omitted. Figure 7 shows the configuration of hydrogen transports and its allocated generation sites to the demand centres.

As technological advancements in electrolysers and the development of renewable energy sources continue, hydrogen becomes increasingly economically viable, leading to a marked reduction in the total levelized cost of hydrogen. These can be observed in Table 4. In Scenario 1, the price of hydrogen has decreased from NZD27.82/kgH_2 to NZD26.94/kgH_2, eventually reaching NZD26.38/kgH_2. Similarly, the price in Scenario 2 started from NZD8.21/kgH_2 and fell to NZD7.16/kgH_2, finally settling at NZD6.56/kgH_2. The cost reduction trend underscores the impact of technological learning rates and renewable energy advancements on reducing hydrogen production costs.

To assess the robustness of the optimization model for Scenario 2, grid electricity prices spanning from 2019 to 2023 have been incorporated into the sensitivity analysis. This approach is justified as electricity from the grid accounts for approximately 20% of the levelized cost of hydrogen. The inclusion is based on the premise that the price of electricity fluctuates monthly, irrespective of the year under consideration. According to the findings in Figure 6, the sensitivity analysis demonstrates that the levelized cost of hydrogen remains largely stable and not highly impacted by the variability in grid electricity pricing.

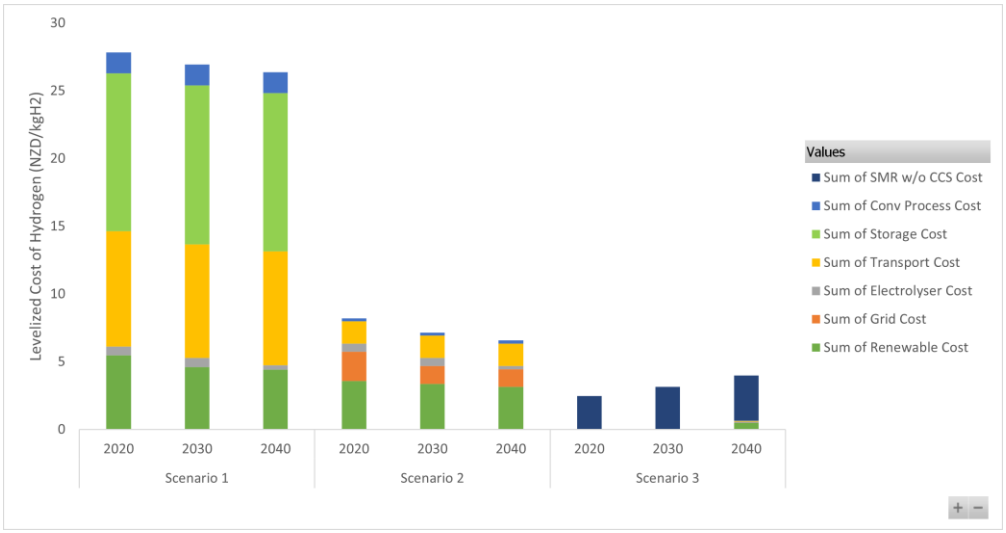

Figure 5. Estimated levelized cost of hydrogen in different case studies from the timeline of 2020 to 2040.

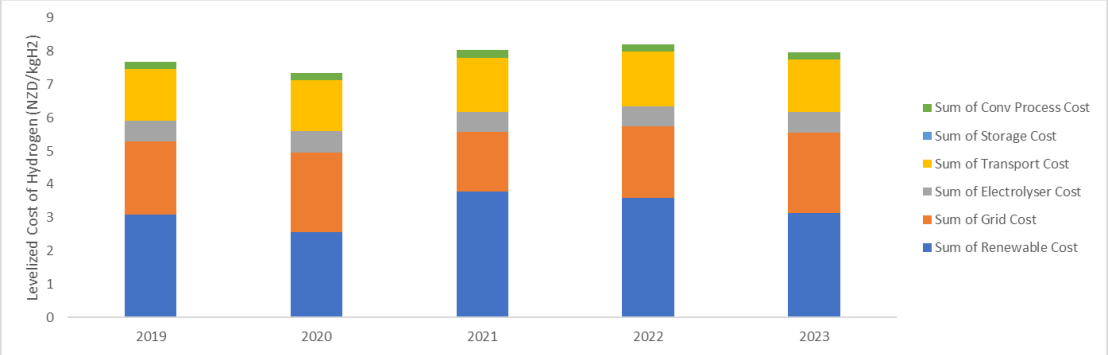

Figure 6. Sensitivity analysis for the levelized cost of hydrogen in Scenario 2 for the base year 2020.

Table 4. Levelized cost of renewables from the timeline of 2020 to 2040 by location.

Index, i	Site Name	Types of Generation	Levelized Cost of Hydrogen (NZD/kgH_2)		
			2020	2030	2040
1	Taheke-Okere Falls Rotoiti	Geothermal	101.68	89.86	86.65
2	Ngatamariki OEC5-Taupo	Geothermal	101.68	89.86	86.65
3	Te Huka Unit 3 - Taupo	Geothermal	101.68	89.86	86.65
4	Geofutures - Te Mihi unit 3	Geothermal	101.68	89.86	86.65
5	Tauhara-Taupo & Tauhara II	Geothermal	101.68	89.86	86.65
6	Kawerau TOP2	Geothermal	101.68	89.86	86.65
7	Rotoma	Geothermal	101.68	89.86	86.65
8	Rangitaiki	Solar	94.55	56.15	51.56
9	Lodestone Three	Solar	89.19	52.96	48.63
10	Ruakākā Solar Farm	Solar	88.96	52.82	48.51
11	Pukenui	Solar	87.50	51.96	47.72
12	Lodestone Five	Solar	88.01	52.26	47.99
13	Lodestone One	Solar	88.33	52.45	48.17
14	Waikato Offshore Wind	Wind	93.55	69.80	63.55
15	South Taranaki Offshore	Wind	63.55	47.41	43.17
16	Kaiwaikawe	Wind	74.55	55.62	50.64
17	Taumatatotara	Wind	103.47	77.20	70.29
18	Awhitu	Wind	90.07	67.20	61.19
19	Taharoa	Wind	100.86	75.25	68.52
20	Kaimai Wind Farm	Wind	156.13	116.48	106.06
21	Puketoi	Wind	67.00	49.99	45.52
22	Project Huriwaka	Wind	70.62	52.69	47.98
23	Turitea	Wind	74.12	55.30	50.35
24	Central Wind (Moawhango)	Wind	102.93	76.80	69.93
25	Waverley	Wind	65.36	48.76	44.40
26	Castle Hill Wind Farm	Wind	65.79	49.08	44.69
27	Puketoi	Wind	67.13	50.08	45.60
28	Rototuna	Wind	70.41	52.53	47.83
29	Castle Hill	Wind	68.21	50.89	46.34

Year	Scenario 1	Scenario2
2020	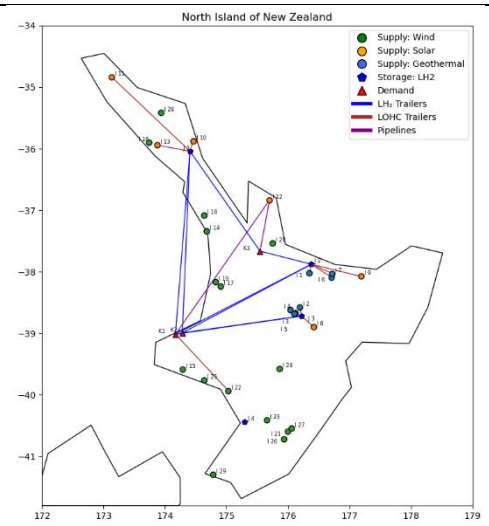 (a)	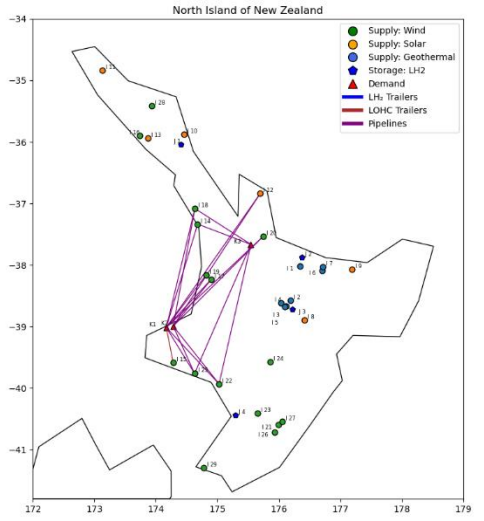 (b)
2030	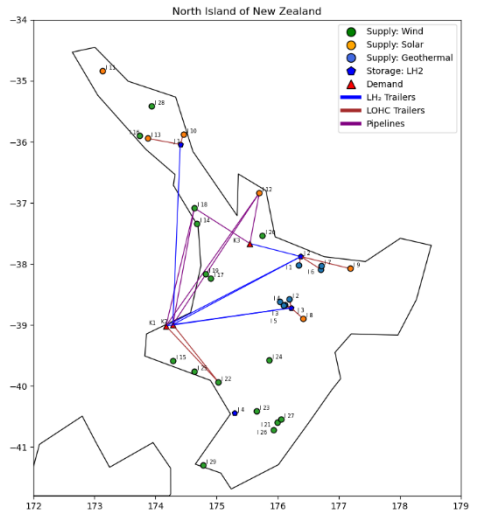 (c)	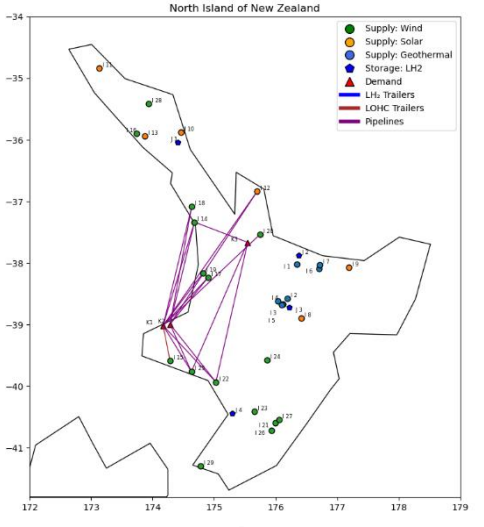 (d)
2040	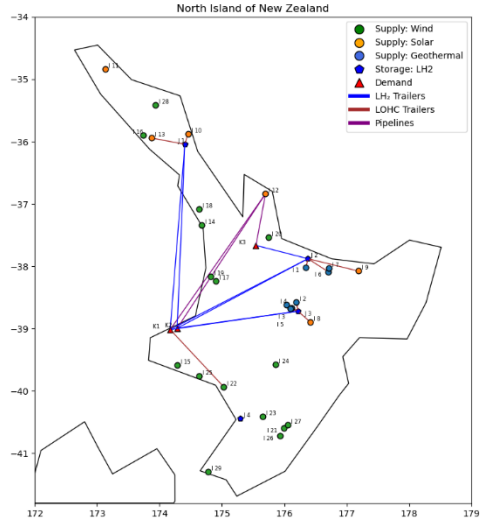 (e)	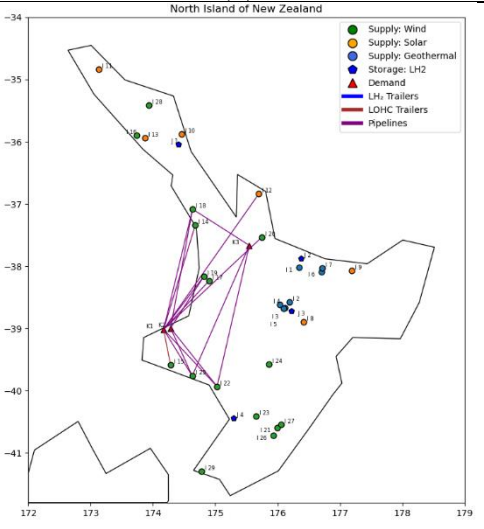 (f)

Figure 7. Configurations of connection between generation, storage and demands sites in Scenario 1 and Scenario 2 at different timelines.

Timeline in Scenario 3

The third scenario includes the existence of steam methane reforming method which is currently used in all of the chemical industries to date. Scenario 3 makes the interaction between green hydrogen from electrolysis with steam methane reforming concerning different timelines. As the carbon cost and natural gas are expected to surge steadily in the future, due to the depletion of fossil fuel reserves and carbon emission targets, it is worth investigating the cost competitiveness of green hydrogen in the scenarios.

Based on the results shown, steam methane reforming technology is wholly used in both years of 2020 and 2030 because the cost of grey hydrogen produced is still much lower than the cost incurred by electrolysis-based hydrogen despite the drastic increase in the shadow price of carbon. However, in 2040, four electricity generation sites (i.e. *I12, I20, I22, I25*) with all having a levelized cost of electricity of lower than NZD50/MWh have been proposed by the model for green hydrogen production (Figure 8). The optimal solution recommends the use of hydrogen pipelines for transporting hydrogen from generation sites to demand centres. Nevertheless, 80.6% or 11252 tonnes monthly of hydrogen is still derived from non-renewable pathway while the remainer is produced from PEM electrolysers. The combined levelized cost of hydrogen is NZD3.97/kgH_2. Therefore, it is economically viable for the uptake of green hydrogen to be used as feedstocks in industries beyond 2040.

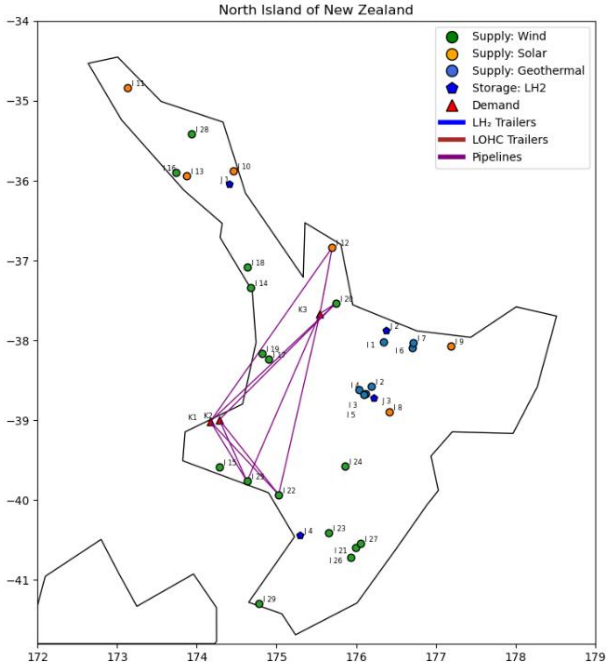

Figure 8. Configurations of connection between generation, storage and demands sites in Scenario 3 at 2040.

CONCLUSION

This study introduces a multi-period Pyomo optimization framework for incorporating a hydrogen supply chain network within the chemical industries on New Zealand's North Island. A Mixed-Integer Linear Programming (MILP) model is developed, capturing the dynamics of intermittent renewable energy sources (i.e. specifically wind and solar power) and the viability of hydrogen storage for industrial use. The model offers quantitative insights into the techno-economic feasibility of green hydrogen across various timelines in New Zealand, assessing different electrolysers, storage solutions, and transportation methods linked to distinct conversion pathways.

The findings highlight the pivotal role of electricity pricing in determining the levelized cost of hydrogen, noting the impracticality of seasonal hydrogen facilities due to high capital costs in Scenario 1. The analysis of a Scenario 2 suggests that, with the advancement of renewable technologies, green hydrogen could become cost-competitive after 2040. Among renewable sources, wind power is identified as the most cost-effective, followed by solar and geothermal energy.

The study also reveals a significant cost difference between the levelized cost of green hydrogen and grey hydrogen, emphasizing the necessity for substantial carbon pricing adjustments and incentives for industries to shift towards renewable resources. In terms of transport, LOHC trailers and compressed gas pipelines are identified as relatively cost-effective methods, with LOHC trailers being more suitable for short distances and small payloads, and pipelines more economical for longer distances and larger volumes.

Future research includes exploring alternative power-to-hydrogen pathways such as biomass, biological fermentation, and photocatalysis. Applying the proposed model to analyse other sectors or industries could broaden its scope. Furthermore, examining the flexibility of the National Grid and hydrogen infrastructure in response to uncertain hydrogen demand at a higher time resolution could enhance the stability of hydrogen production.

ACKNOWLEDGEMENT

This research has been supported by the programme “Ahuora: Centre for Smart Energy Systems”, an Advanced Energy Technology Platform, funded by the New Zealand Ministry of Business, Innovation and Employment.

SUPPLEMENTARY MATERIAL

Additional materials will be provided if requested.

NOMENCLATURE

Indices and Sets

Sets

$t \in T$	Monthly time period
$i \in I$	Number of generation sites
$r \in R$	Types of renewable technologies
$st \in St$	Types of storage technologies
$j \in J$	Number of intermediate storage sites
$tr \in Tr$	Types of transport technologies
$k \in K$	Number of demand sites
$p \in P$	Types of conversion module
$p_4 \in P_4$	Pathways of conversion module from transport to storage

Mass Balance

Parameters

Cap_{ir}^{ir}	Available capacity of type of renewable technology r at location i
UF_r	Utilization factor for renewable technology r
X_e^e	Conversion factor for electrolyser technology e
X_p^{p1}	Conversion factor that accounts for process losses for process p in process step 1
X_p^{p2}	Conversion factor for process p in process step 2
$NIP2Tr_{p,tr}$	Pathway connection node for process p in process step 2 with transport mode tr
$X_{tr,p,p4,st}^{trp3}$	Conversion factor for process step 3 when transport mode tr, process p in process step 3, process $p4$ in process step 4 and storage mode st is applied
$X_{tr,p,p4,st}^{trp3p4st}$	Conversion factor for storage amount when transport mode tr, process p in process step 3, process $p4$ in process step 4 and storage mode st is applied
X_{st}^{st}	Conversion factor that accounts for storage losses for storage technology st
$NKTrP5_{tr,p}$	Pathway connection node for transport mode tr with process p in process step 5
$DEM_{k,t}$	Hydrogen demand at location k at time period t
X_{tr}^{tr}	Conversion factor for transport mode tr
DEM^{Total}	Total hydrogen demand required for all demand centres

Non-Negative Variables

$FIR_{i,r}^{Cap}$	Capacity of type of renewable technology r at location i
$FIR_{i,r,t}^{rated}$	Rate at which rated electricity power at location i with renewable technology r during time t
$FI1_{i,t}$	Rate at which electricity is generated at location i during time t
$FIR_{i,r,t}$	Rate at which electricity is generated at location i with renewable technology r during time t
$FI2_{i,t}$	Rate at which the electricity resource is present at location i during time t

$FI_{i,t}^{grid}$	Rate at which the electricity is obtained from the grid at location i during time t
$FI_{i,t}^{excess}$	Rate at which the excess electricity resource is sent to the grid at location i during time t
$FI3_{i,t}$	Net rate of electricity resource balance at location i during time t
$FIE_{i,e,t}$	Rate at which the hydrogen is generated from electrolyser type e at location i during time t
$Cap_{i,e}^{ie}$	Maximum capacity of electrolyser type e in location i
$FI4_{i,t}$	Rate at which hydrogen is generated at location i during time t
$FIP1_{i,p,t}$	Rate at which hydrogen is available from process type (P1) p at location i during time t
$FIP2_{i,p,t}$	Rate at which hydrogen is available from process type (P2) p at location i during time t
$FIP2Tr_{i,p,tr,t}$	Rate at which hydrogen is available for transport mode tr from process type (P2) p at location i during time t
$FITr_{i,tr,t}$	Rate at which hydrogen is available for transport mode tr at location i during time t
$FIJTr_{i,j,tr,t}$	Rate at which hydrogen is delivered with transport mode tr between location source i and storage site j during time t
$FIKTr_{i,k,tr,t}$	Rate at which hydrogen is delivered with transport mode tr between location source i and demand centre k during time t
$FJTr_{j,tr,t}^{in}$	Rate at which hydrogen is delivered with transport mode tr to storage site j during time t
$FJTrP3_{j,tr,p,p4,st,t}$	Rate at which hydrogen is available after process step 3 when transport mode tr, process p in process step 3, process $p4$ in process step 4 and storage mode st is applied
$FJTrP3P4St_{j,tr,p,p4,st,t}$	Rate at which hydrogen is available in storage when transport mode tr, process p in process step 3, process $p4$ in process step 4 and storage mode st is applied
$FJSt_{j,st,t}^{in}$	Rate at which hydrogen entering storage module st at storage site j during time t
$FJ_{j,t}^{in}$	Rate at which hydrogen entering storage site j during time t
$FJSt_{j,st,t}^{out}$	Rate at which hydrogen leaving storage module st at storage site j during time t
$FJ_{j,st,t}^{out}$	Rate at which hydrogen leaving storage site j during time t
$I_{j,st,t}^{FJSt}$	The inventory balance for storage facility st at storage site j at time t
$I_{j,st}^{Cap}$	Maximum capacity of storage facility st in storage site j
$FJStTr_{j,st,tr,t}$	Rate at which hydrogen is available for transport mode tr from storage facility st at storage site j during time t
$FJTr_{j,tr,t}^{out}$	Rate at which hydrogen is available for transport mode tr at storage site j during time t
$FJKTr_{j,k,tr,t}$	Rate at which hydrogen is delivered with transport mode tr between storage site j and demand centre k during time t
$FKTr_{k,tr,t}$	Rate at which hydrogen is delivered with transport mode tr to demand centre k during time t
$FKTrP5_{k,tr,p,t}$	Rate at which hydrogen is available after process step (P5) p with transport mode tr at demand centre k during time t

$FK_{k,t}$	Rate at which hydrogen is available at demand centre k during time t
$FK_{k,t}^{SMR}$	Rate at which hydrogen is produced from at demand centre k during time t
$FK_{k,t}^{smr_{CO2}}$	Rate at which hydrogen is produced by SMR at demand centre k during time t

Integer Variables

N_i^T	Number of wind turbines for each specific location i
$N_{i,j}^{trips}$	Maximum number of trips taken by a truck between location i to location j at a time period
$N_{j,k}^{trips}$	Maximum number of trips taken by a truck between location j to location k at a time period
$N_{i,k}^{trips}$	Maximum number of trips taken by a truck between location i to location k at a time period
$N_{i,j,tr}^{vehicles}$	Number of vehicles needed to travel from location i to location j with transport type tr
$N_{j,k,tr}^{vehicles}$	Number of vehicles needed to travel from location j to location k with transport type tr
$N_{i,k,tr}^{vehicles}$	Number of vehicles needed to travel from location i to location k with transport type tr

Binary Variables

$BI_{i,t}^{excess}$	Availability of excess electricity resource is sent to the grid at location i during time t
$BI_{i,t}^{grid}$	Availability of electricity is obtained from the grid at location i during time t
$BIE_{i,e}$	Availability of electrolyser technology e employed at location i
$BIP1_{i,p}$	Establishment of process pathway P1 p at location i
$BIP2Tr_{i,tr}$	Establishment of process pathway P2 p with transport mode tr at location i
$BJTrP3P4St_{j,tr,p,p4,st}$	Establishment of pathway from transport mode tr, process step (P3) p, process step (P4) $p4$ and storage facility st for storage site j
$BJStTr_{j,tr}$	Establishment of pathway from storage and transport at storage site j and transport mode tr

Constants

$\bar{v}_{i,t}$	Rate of wind speed at location i during time t
$CF_{i,r,t}$	Capacity factor of renewable technology r at location i during time t
R	Length of the wind blade
Cp	Coefficient of performance for wind power generation
ρ^{air}	Density of air (kg/m^3)
h	Number of utilisation hours per month
a^{os}	The coefficient of overload capability of the electrolyser

Cost function

Non-Negative Variables

$Capacity^{eq}$	Capacity of a system
$Capacity^{eq,nominal}$	Nominal capacity of a system
$Invest^{ref}$	Investment cost of a referenced system
$Invest^{eq}$	Investment cost of a system
AF	Annuity factor of a system
$CAPEX^{eq}$	Capital expenditure of a system
$OPEX^{eq,fix}$	Fixed operational cost of a system
$throughput$	Throughput of a system
$OPEX^{eq,var}$	Variable operational cost of a system
$Cap_{i,j,tr}^{ijtr}$	Capacity of rate at which hydrogen is delivered with transport mode tr between location source i and storage site j
$Cap_{i,p}^{p1}$	Capacity of rate at which is hydrogen available from process type (P1) p at location i
$Cap_{i,p}^{p2}$	Capacity of rate at which hydrogen is available from process type (P2) p at location i
$Cap_{j,p}^{p3}$	Capacity of rate at which hydrogen is available from process type (P3) p at location j
$Cap_{j,p4}^{p4}$	Capacity of rate at which hydrogen is available from process type (P4) $p4$ at location j
$Cap_{k,p}^{p5}$	Capacity of rate at which is available from process type (P5) p at location k
$invest_{i,j,tr}^{ijtr}$	Investment cost of transport system tr travelling from location i to location j
$invest_{i,p}^{p1}$	Investment cost of process type (P1) p at location i
$invest_{i,p}^{p2}$	Investment cost of process type (P2) p at location i
$invest_{j,p}^{p3}$	Investment cost of process type (P3) p at location j
$invest_{j,p4}^{p4}$	Investment cost of process type (P4) $p4$ at location j
$invest_{k,p}^{p5}$	Investment cost of process type (P5) p at location k
$CAPEX_{k}^{smr}$	Capital expenditure of the SMR at location k
$OPEX_{k}^{smr.fixed}$	Fixed operational cost of the SMR at location k
$OPEX_{k,t}^{smr,var}$	Variable operational cost of the SMR system at location k at time t
CAP_{k}^{smr}	Capacity of rate at which hydrogen is available from SMR at location k
$Cost_{k,t}^{CO2}$	Cost incurred by carbon emission at location k at time t
$LCOE_{i,r}$	Levelized cost of energy for renewable technology r at location i
$TOTEX$	Total expenditure
$TOTEX^{renewable}$	Total expenditure of renewable technologies
$TOTEX^{grid}$	Total expenditure of grid systems
$TOTEX^{etech}$	Total expenditure of electrolyser technologies
$TOTEX^{truckij}$	Total expenditure of trucks travelling from location i to location j
$TOTEX^{transportij}$	Total expenditure of transportations from location i to location j
$TOTEX^{truckjk}$	Total expenditure of trucks travelling from location j to location k
$TOTEX^{transportjk}$	Total expenditure of transportations from location j to location k
$TOTEX^{truckik}$	Total expenditure of trucks travelling from location i to location k

$TOTEX^{transportik}$	Total expenditure of transportations from location i to location k
$TOTEX^{store}$	Total expenditure of storage facilities
$TOTEX^{p1}$	Total expenditure of process type (P1)
$TOTEX^{p2}$	Total expenditure of process type (P2)
$TOTEX^{p3}$	Total expenditure of process type (P3)
$TOTEX^{p4}$	Total expenditure of process type (P4)
$TOTEX^{p5}$	Total expenditure of process type (P5)
$TOTEX^{smr}$	Total expenditure of SMR

Constants

f^{cap}	Overcapacity factor
f^{prod}	Overproduction factor
$invest^{ref}$	Referenced investment cost of a system
$capacity^{ref}$	Referenced capacity of a system
$scale\ factor$	Scale factor
$WACC$	Weighted average cost of capital
n	Depreciation period
OM^{fix}	Fixed operational and maintenance costs
$electricity\ demand^{ref}$	Electricity demand of a referenced system
$electricity\ price^{ref}$	Electricity tariff of a referenced system
$heat\ demand^{ref}$	Heat demand of a referenced system
$heating\ price^{ref}$	Heat tariff of a referenced system
$D_{i,j}^{ij}$	Distance between location i and location j
$D_{j,k}^{jk}$	Distance between location j and location k
$D_{i,k}^{ik}$	Distance between location i and location k
h^{tr}	Utilisation hour of trucks with transport technology tr in a year
v	Travel speed of trucks in km/h
Cap_{tr}^{net}	Net capacity of trailers with transport mode tr
$invest_{tr}^{ref}$	Referenced investment cost of transport mode tr
$demand^{diesel}$	Amount of diesel used for every km
c^{diesel}	Price of diesel per litre
EF	Specific CO2 emissions from SMR process
a^{CO2}	
CRF_r	Capital Recovery Factor
PFF_r	Project Finance factor
$C_r^{OvernightCapitalCost}$	Overnight Capital Cost
$C_r^{FixedOP\&Main}$	Fixed Operation and Maintenance Expenses
$E_r^{VariableOP\&Main}$	Variable Operation and Maintenance Expenses
$\alpha_r^{TaxCredit}$	Tax Credit

REFERENCES

[1] N. Sazali, "Emerging technologies by hydrogen: A review," *International Journal of Hydrogen Energy*, vol. 45, no. 38, pp. 18753–18771, Jul. 2020, doi: 10.1016/j.ijhydene.2020.05.021.

[2] S. Griffiths, B. K. Sovacool, J. Kim, M. Bazilian, and J. M. Uratani, "Industrial decarbonization via hydrogen: A critical and systematic review of developments, socio-technical systems and policy options," *Energy Research & Social Science*, vol. 80, p. 102208, Oct. 2021, doi: 10.1016/j.erss.2021.102208.

[3] Ministry of Business Innovation and Employment, "New Zealand's hydrogen regulatory pathway." Ministry of Business Innovation and Employment, Jul. 15, 2022. [Online]. Available: https://www.mbie.govt.nz/dmsdocument/25671-new-zealand-hydrogen-regulatory-pathway

[4] P. Agnolucci, O. Akgul, W. McDowall, and L. G. Papageorgiou, "The importance of economies of scale, transport costs and demand patterns in optimising hydrogen fuelling infrastructure: An exploration with SHIPMod (Spatial hydrogen infrastructure planning model)," *International Journal of Hydrogen Energy*, vol. 38, no. 26, pp. 11189–11201, Aug. 2013, doi: 10.1016/j.ijhydene.2013.06.071.

[5] S. De-León Almaraz, C. Azzaro-Pantel, L. Montastruc, and S. Domenech, "Hydrogen supply chain optimization for deployment scenarios in the Midi-Pyrénées region, France," *International Journal of Hydrogen Energy*, vol. 39, no. 23, pp. 11831–11845, Aug. 2014, doi: 10.1016/j.ijhydene.2014.05.165.

[6] N. V. S. N. Murthy Konda, N. Shah, and N. P. Brandon, "Optimal transition towards a large-scale hydrogen infrastructure for the transport sector: The case for the Netherlands," *International Journal of Hydrogen Energy*, vol. 36, no. 8, pp. 4619–4635, Apr. 2011, doi: 10.1016/j.ijhydene.2011.01.104.

[7] S. Samsatli, I. Staffell, and N. J. Samsatli, "Optimal design and operation of integrated wind-hydrogen-electricity networks for decarbonising the domestic transport sector in Great Britain," *International Journal of Hydrogen Energy*, vol. 41, no. 1, pp. 447–475, Jan. 2016, doi: 10.1016/j.ijhydene.2015.10.032.

[8] M. Pfennig *et al.*, "Global GIS-based potential analysis and cost assessment of Power-to-X fuels in 2050," *Applied Energy*, vol. 347, p. 121289, Oct. 2023, doi: 10.1016/j.apenergy.2023.121289.

[9] Alessandro Guzzini, Giovanni Brunaccini, Davide Aloisio, Marco Pellegrini, Cesare Saccani, and Francesco Sergi, "A New Geographic Information System (GIS) Tool for Hydrogen Value Chain Planning Optimization: Application to Italian Highways," *Sustainability*, vol. 15, no. 3, p. 2080, 2023, doi: https://doi.org/10.3390/su15032080.

[10] S. Almaraz, C. Azzaro-Pantel, L. Montastruc, L. Pibouleau, and O. Senties, "Assessment of mono and multi-objective optimization to design a hydrogen supply chain," *International Journal of Hydrogen Energy*, vol. 38, pp. 14121–14145, Nov. 2013, doi: 10.1016/j.ijhydene.2013.07.059.

[11] M. Moreno-Benito, P. Agnolucci, and L. G. Papageorgiou, "Towards a sustainable hydrogen economy: Optimisation-based framework for hydrogen infrastructure development," *Computers & Chemical Engineering*, vol. 102, pp. 110–127, Jul. 2017, doi: 10.1016/j.compchemeng.2016.08.005.

[12] B. van der Heijde, A. Vandermeulen, R. Salenbien, and L. Helsen, "Representative days selection for district energy system optimisation: a solar district heating system with seasonal storage," *Applied Energy*, vol. 248, pp. 79–94, Aug. 2019, doi: 10.1016/j.apenergy.2019.04.030.

[13] S. Samsatli and N. Samsatli, "The role of renewable hydrogen and inter-seasonal storage in decarbonising heat – Comprehensive optimisation of future renewable energy value

chains," *Applied Energy*, vol. 233–234, pp. 854–893, Jan. 2019, doi: 10.1016/j.apenergy.2018.09.159.
[14] S. Shirazaki, M. S. Pishvaee, and M. A. Sobati, "Integrated supply chain network design and superstructure optimization problem: A case study of microalgae biofuel supply chain," *Computers & Chemical Engineering*, vol. 180, p. 108468, Jan. 2024, doi: 10.1016/j.compchemeng.2023.108468.
[15] S. Poletti and I. Staffell, "Understanding New Zealand's wind resources as a route to 100% renewable electricity," *Renewable Energy*, vol. 170, pp. 449–461, Jun. 2021, doi: 10.1016/j.renene.2021.01.053.
[16] M. J. Barasa Kabeyi and O. A. Olanrewaju, "Geothermal wellhead technology power plants in grid electricity generation: A review," *Energy Strategy Reviews*, vol. 39, p. 100735, Jan. 2022, doi: 10.1016/j.esr.2021.100735.
[17] R. Gelaro *et al.*, "The Modern-Era Retrospective Analysis for Research and Applications, Version 2 (MERRA-2)," *Journal of Climate*, vol. 30, no. 14, pp. 5419–5454, Jul. 2017, doi: 10.1175/JCLI-D-16-0758.1.
[18] H. Hersbach *et al.*, "The ERA5 global reanalysis," *Quarterly Journal of the Royal Meteorological Society*, vol. 146, no. 730, pp. 1999–2049, 2020, doi: 10.1002/qj.3803.
[19] S. Kobayashi *et al.*, "The JRA-55 Reanalysis: General Specifications and Basic Characteristics," *Journal of the Meteorological Society of Japan*, vol. 93, no. 1, pp. 5–48, 2015, doi: 10.2151/jmsj.2015-001.
[20] L. Moraes, C. Bussar, P. Stoecker, K. Jacqué, M. Chang, and D. U. Sauer, "Comparison of long-term wind and photovoltaic power capacity factor datasets with open-license," *Applied Energy*, vol. 225, pp. 209–220, Sep. 2018, doi: 10.1016/j.apenergy.2018.04.109.
[21] I. McCarthy and H. O. Balli, "Windfarms and residential property values," *International Journal of Strategic Property Management*, vol. 18, no. 2, pp. 116–124, Apr. 2014, doi: 10.3846/1648715X.2014.889770.
[22] National Renewable Energy Laboratory, "Annual Technology Baseline." National Renewable Energy Laboratory, 2022. [Online]. Available: https://atb.nrel.gov/
[23] A. H. Reksten, M. S. Thomassen, S. Møller-Holst, and K. Sundseth, "Projecting the future cost of PEM and alkaline water electrolysers; a CAPEX model including electrolyser plant size and technology development," *International Journal of Hydrogen Energy*, vol. 47, no. 90, pp. 38106–38113, Nov. 2022, doi: 10.1016/j.ijhydene.2022.08.306.
[24] Hydrogen Council, "Path to Hydrogen Competitiveness," Hydrogen Council, Jan. 2020. [Online]. Available: https://hydrogencouncil.com/wp-content/uploads/2020/01/Path-to-Hydrogen-Competitiveness_Full-Study-1.pdf
[25] M. Kopp, D. Coleman, C. Stiller, K. Scheffer, J. Aichinger, and B. Scheppat, "Energiepark Mainz: Technical and economic analysis of the worldwide largest Power-to-Gas plant with PEM electrolysis," *International Journal of Hydrogen Energy*, vol. 42, no. 19, pp. 13311–13320, May 2017, doi: 10.1016/j.ijhydene.2016.12.145.
[26] J. Park *et al.*, "Green hydrogen to tackle the power curtailment: Meteorological data-based capacity factor and techno-economic analysis," *Applied Energy*, vol. 340, p. 121016, Jun. 2023, doi: 10.1016/j.apenergy.2023.121016.
[27] J. Andersson and S. Grönkvist, "Large-scale storage of hydrogen," *International Journal of Hydrogen Energy*, vol. 44, no. 23, pp. 11901–11919, May 2019, doi: 10.1016/j.ijhydene.2019.03.063.
[28] Agata Godula-Jopek, Walter Jehle, and Jörg Wellnitz, "Storage of Pure Hydrogen in Different States," in *Hydrogen Storage Technologies*, John Wiley & Sons, Ltd, 2012, pp. 97–170. doi: 10.1002/9783527649921.ch4.

[29] M. Klell, “Storage of Hydrogen in the Pure Form,” in *Handbook of Hydrogen Storage: New Materials for Future Energy Storage*, Germany: John Wiley & Sons, Ltd, 2010, pp. 1–37. doi: 10.1002/9783527629800.ch1.
[30] Land Information New Zealand, “Land Information New Zealand.” [Online]. Available: https://www.linz.govt.nz/
[31] Stats NZ, “Stats NZ.” [Online]. Available: https://datafinder.stats.govt.nz/
[32] GNS Science, “GNS Science.” [Online]. Available: https://www.gns.cri.nz/
[33] M. Reuß, T. Grube, M. Robinius, P. Preuster, P. Wasserscheid, and D. Stolten, “Seasonal storage and alternative carriers: A flexible hydrogen supply chain model,” *Applied Energy*, vol. 200, pp. 290–302, Aug. 2017, doi: 10.1016/j.apenergy.2017.05.050.
[34] T. Wlodek, S. Kuczyński, A. Olijnyk, M. Łaciak, and A. Szurlej, “Thermodynamic and Technical Issues of Hydrogen and Methane-Hydrogen Mixtures Pipeline Transmission,” *Energies*, vol. 12, p. 569, Feb. 2019, doi: 10.3390/en12030569.
[35] Dennis Krieg, “Wasserstofftransport per Pipeline in Deutschland,” in *Konzept und Kosten eines Pipelinesystems zur Versorgung des deutschen Straßenverkehrs mit Wasserstoff*, vol. 144, Forschungszentrum Jülich, 2012.

APPENDIX

Wlodek et al. [34] estimates the size of diameter based on the flow rate of hydrogen at a specific time. Krieg [35] calculates the pipe investment cost per metre as a function of distance. As the pipe investment cost per unit distance is a polynomial equation which is influenced by the diameter of the pipe, the equation is represented by a piecewise linear function to ensure an optimal solution.

$$f_{tr}^{pipelines}(Cap_{i,j,tr}^{ijtr}) = \begin{cases} m_1 \cdot Cap_{i,j,tr}^{ijtr} + c_1, & a_1 < Cap_{i,j,tr}^{ijtr} \leq b_1, \forall i \in I, \forall j \in J \\ m_2 \cdot Cap_{i,j,tr}^{ijtr} + c_2, & a_2 < Cap_{i,j,tr}^{ijtr} \leq b_2, \forall i \in I, \forall j \in J \\ m_n \cdot Cap_{i,j,tr}^{ijtr} + c_n, & a_n < Cap_{i,j,tr}^{ijtr} \leq b_n, \forall i \in I, \forall j \in J \\ & \dots \end{cases} \quad \text{(A1)}$$

Table A 1. Piecewise coefficient for investment cost for pipelines.

Index,n	m_n	c_n	a_n	b_n
1	3.115	0	0	125
2	1.575	192.5	125	200
3	1.85	137.5	200	250
4	2.07	82.5	250	300
5	2.29	16.5	300	350

The hydrogen supply chain is a sophisticated network which includes several technologies and processes which are concurrently existing in each location. Each site might exhibit different technologies depending on the location and the availability of resources within the region, hence the selection of facility in each unit is independent on one another although it is associated with the minimization of levelized cost of hydrogen. In Appendix B, the general assumptions and values used for the optimisation model will be listing in its respective tables. Table A 2 reveals the assumed efficiency from the improvement rate from the development of electrolyser corresponding to the timeline.

Table A 3 and Table A 4 illustrate the assumption made for the transport technologies. The conversion assumptions for all conversion modules for all process steps are displayed in Table A 6.

Table A 2. Assumptions on electrolyser technologies [25].

Electrolyser	AEL	PEM Electrolyser
Efficiency (2020)	0.70	0.60
Efficiency (2030)	0.70	0.65
Efficiency (2040)	0.70	0.69
Depreciation Period, year	25	15
Annuity Factor, AF	9.4%	11.7%

Table A 3. Assumptions made for transport modes [33].

Supply	Pipeline	Trailer GH_2	Trailer LH_2	Trailer LOHC
$Invest_{tr}^{ref,tr}$	Eqn(A1)	962.5 kNZD	1,505 kNZD	262.5 kNZD
Depreciation Period, n	40 years	12 years	12 years	12 years
OM_{tr}	4%	2%	2%	2%
Design Capacity	-	0.67	4.3	1.8
Losses	0.5%	0.5%	3%	0.5%
$electricity\ demand_{tr}^{ref,tr}$	2.0 MWh/ton	1.9 MWh/ton	0.6 MWh/ton	4.4 MWh/ton
$heat\ demand_{tr}^{ref,tr}$	-	-	-	9 MWh/ton

Table A 4. Assumptions made for trucks [33].

Truck	
$Invest_{tr}^{tr0}$	NZD 280,000
Depreciation Period, n	8
Hour of utilisation per year, h^{tr}	2000 h/year
Fixed operational & maintenance costs, OM^{fix}	12%
Diesel Demand	35 l/100 km
Speed	50 km/h
Diesel c_{diesel}	2.12 NZD/L

Table A 5. Potential sites for hydrogen storage.

Index	Region	Latitude	Longitude
101	Northland	-36.04	174.41
102	Bay of Plenty	-37.88	176.38
103	Taupo	-38.72	176.22
104	Manawatu-Wanganui-Wellington	-40.44	175.29

Table A 6. Assumptions on conversion technologies [33].

	Compression	Liquefaction	Hydrogenation	Dehydrogenation	LH_2 Pump	LOHC Pump	Evaporation
$State_{in}$	GH_2	GH_2	GH_2	LOHC	LH_2	LOHC	LH_2
$State_{out}$	GH_2	LH_2	LOHC	GH_2	LH_2	LOHC	GH_2
$Invest_p^{ref}$	6.8 kNZD	184 MNZD	70 MNZD	52.5 MNZD	52.5	87.5	10.5 kNZD
$Capacity_p^{ref}$	0.44 ton/month	1500 ton/month	9000 ton/month	9000 ton/month	0.03 ton/month	30 ton/month	30 ton/month
Scale factor	0.8335	0.66	0.6	0.6	1	1	1
Depreciation $Period_p$	15 y	20 y	10 y	20 y	10 y	10 y	10 y
OM_p	4%	8%	3%	3%	3%	3%	3%
Electricity $demand_p^{ref}$	0.6035 MWh/ton	6.78 MWh/ton	0.37 MWh/ton	0.37 MWh/ton	0.1 MWh/ton	0.1 MWh/ton	0.6 MWh/ton
Heat $demand_p^{red}$	-	-	-9 MWh/ton	9 MWh/ton	-	-	-
Losses	0.5%	1.65%	3%	1%	-	-	-